Photoinduced Intramolecular Electron-Transfer Processes in [60]Fullerene-(Spacer)-*N,N*-Bis(biphenylyl)aniline Dyad in Solutions

G. Abraham Rajkumar,[†,¶] Atula S. D. Sandanayaka,[‡] Kei-ichiro Ikeshita,[†] Mitsunari Itou,[‡] Yasuyuki Araki,[‡] Yoshio Furusho,[†,£] Nobuhiro Kihara,[†] Osamu Ito,[‡,*] and Toshikazu Takata*[*,†,¶]

Department of Applied Chemistry, Osaka Prefecture University, Gakuen-cho, Sakai-shi, Osaka 599-8531, Japan, Department of Organic and Polymeric Materials, Tokyo Institute of Technology, Ookayama, Meguro, Tokyo 152-8552, Japan, Yashima Super Structured-Helix Project, JST, Moriyama-ku, Nagoya 463-0003, Japan, and Institute of Multidisciplinary Research for Advanced Materials, Tohoku University, Katahira 2-1-1, Aoba-ku, Sendai 980-8577, Japan

Received: July 14, 2004; In Final Form: November 30, 2004

Intramolecular photoinduced charge-separation and charge-recombination processes in a covalently connected C_{60}-(spacer)-*N,N*-bis(biphenylyl)aniline (C_{60}-spacer-BBA) dyad, in which the center-to-center distance of the electron acceptor and electron donor is 15 Å, have been studied by time-resolved fluorescence and transient absorption methods. The observed low fluorescence intensity and the short fluorescence lifetime of the C_{60} moiety of the dyad in PhCN and THF indicate that charge separation takes place via the excited singlet state of the C_{60} moiety at a quite fast rate and a high efficiency. The nanosecond transient absorption spectra in PhCN and THF showed the broad absorption bands at 880 and 1100 nm, which were attributed to $C_{60}^{\bullet-}$-spacer-BBA$^{\bullet+}$. The charge-separated state decays with a lifetime of 330−360 ns in PhCN and THF at room temperature. From temperature dependence of the charge-recombination rate constants, the reorganization energy was evaluated to be 0.77−0.87 eV, which indicates that the charge-recombination process is in the inverted region of the Marcus parabola. With lowering temperature, the contribution of charge separation via the excited triplet state of the C_{60} moiety increases due to an increase in solvation of $C_{60}^{\bullet-}$-spacer-BBA$^{\bullet+}$.

Introduction

Because [60]fullerene, C_{60}, has been revealed as a very attractive electron acceptor with unique photophysical and electrochemical properties,[1−3] considerable efforts have been devoted in recent years to develop the systems in which C_{60} is covalently linked to electron donors,[4−12] in addition to the mixture systems of C_{60} and donor.[14−21] Molecular systems including C_{60} are of particular interest, because they can exhibit characteristic electronic properties in the excited states in addition to its small reorganization energy due to spherical molecular shape;[22] thus, a lot of research has been conducted to the photoinduced electron-transfer processes including C_{60}.[23−25] These phenomena open the potential applications in the realization of new artificial photosynthetic systems, molecular electronic devices, and photovoltaic cells.[4,6,7]

Among the wide variety of donor molecules that can be covalently linked to C_{60}, one of the fascinating donors is aromatic amines; various aromatic amine-connected C_{60} dyads have been synthesized and the photoinduced processes were revealed.[5] In the previous report, it was reported that C_{60}-bis(biphenylyl)aniline (BBA) dyad with a short linkage with a center-to-center distance (R_{CC} of C_{60}-BBA) of 10 Å generates a quite persistent charge-separated state in PhCN even in such a short distance between the radical anion and radical cation.[26]

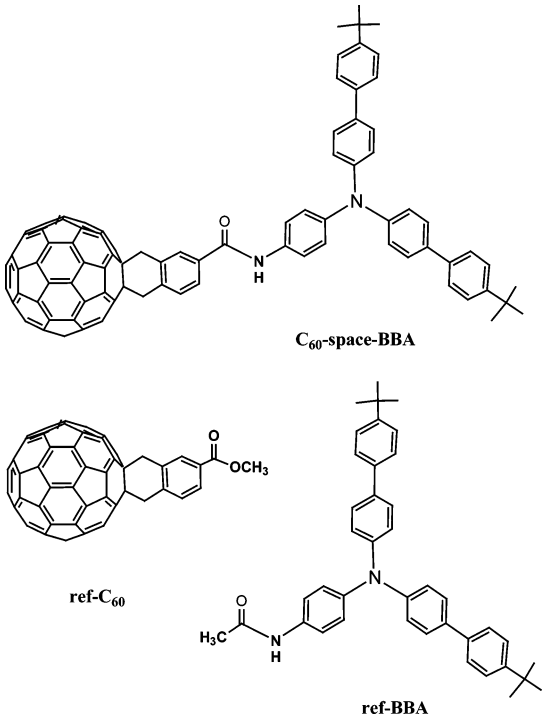

Figure 1. Molecular structures of C_{60}-spacer-BBA and reference samples.

In the present study, we report synthesis of C_{60}-spacer-BBA dyad with a longer linkage (R_{CC} = 15 Å), as shown in Figure 1 and the charge-separation and charge-recombination processes

* Author for correspondence. E-mail: takata@chem.osakafu-u.ac.jp. E-mail: ito@tagen.tohoku.ac.jp.
† Osaka Prefecture University.
¶ Tokyo Institute Technology.
£ Yashima Super Structured Helix Project.
‡ Tohoku University.

10.1021/jp046879c CCC: $30.25
Published on Web 02/19/2005

SCHEME 1

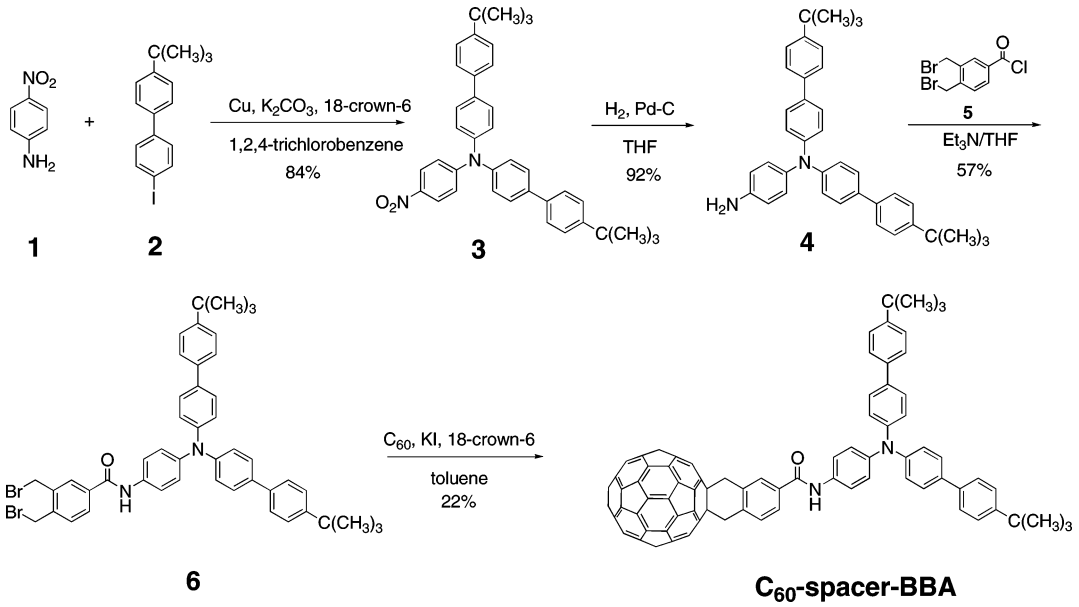

investigated by the time-resolved fluorescence and absorption spectra in the visible and near-IR regions. It would be expected that the temperature effects on the rate constants of the charge-separation and charge-recombination processes afford valuable information about the Marcus parameters of the electron-transfer processes of this dyad.[27]

Results and Discussion

Synthesis of C_{60}-Spacer-BBA. C_{60}-spacer-BBA was synthesized as shown in Scheme 1. The Ullmann coupling of 4-nitroaniline **1** with 4-*tert*-butyl-4′-iodobiphenyl (**2**) in 1,2,4-trichlorobenzene using Cu powder as a catalyst afforded triarylamine **3** in 84% yield. Nitroarene **3** was subjected to the catalytic hydrogenation using Pd/C to give amine **4** in 92% yield. Reaction of **4** with acid chloride **5** gave amide **6** in 57% yield. Diels−Alder reaction of **6** and C_{60} in refluxing toluene afforded C_{60}-spacer-BBA in 22% yield. The structure of C_{60}-spacer-BBA was fully characterized by ^{1}H and ^{13}C NMR, IR, and elemental analysis. Ref-BBA was prepared according to the literature method.[28] Reaction of **4** with acetyl chloride in the presence of an amine gave ref-BBA in 75% yield. Ref-C_{60}, which is 4-methoxycarbonyl-*o*-quinodimethane adduct with C_{60}, was prepared according to the method described in the literature.[29] Details are described in the Experimental Section.

Molecular Orbital Calculations. Figure 2 shows the optimized structure, the electron densities of the lowest unoccupied molecular orbital (LUMO), and the highest occupied molecular orbital (HOMO) of C_{60}-spacer-BBA dyad calculated by *GAUSSIAN 98* at the B3LYP/3-21G level.[30] The optimized structure shows that relative positions of BBA and C_{60} with $R_{CC} = 15$ Å, in which the BBA plane is in the same plain with the bridge bonds, but not face-to-face alignment with the C_{60} sphere. The calculated electron densities of the HOMO indicate the delocalization of electrons in the BBA moiety, whereas the electron densities in the LUMO are all located on the C_{60} moiety, suggesting that the BBA and C_{60} moieties act as an electron-donor and an electron-acceptor, respectively.

Electrochemical Measurements. The cyclic voltammogram of C_{60}-spacer-BBA dyad in PhCN is shown in Figure 3. Almost reversible pattern was observed, suggesting the stability of the radical ions. The E_{ox} value (0.33 V vs Fc/Fc$^+$) of C_{60}-spacer-BBA was almost the same as the E_{ox} values of ref-BBA ($E_{ox} = +0.35$ V vs Fc/Fc$^+$), suggesting the absence of interaction between BBA and C_{60} in the ground state.

The reduction potential (E_{red}) of C_{60}-spacer-BBA was evaluated to be -1.02 V vs Fc/Fc$^+$; this value is corresponding to E_{red} of the C_{60} moiety, because a quite similar value was reported for the ref-C_{60} ($E_{red} = -1.10$ V vs Fc/Fc$^+$).[7c] From these E_{ox} and E_{red} values for BBA-spacer-C_{60}, the free-energy changes for charge separation (ΔG_{CS}) and charge recombination (ΔG_{CR}) can be calculated from the Weller equations:[31]

$$-\Delta G_{CS} = \Delta E_{0-0} - (-\Delta G_{CR}) \quad (1)$$

$$-\Delta G_{CR} = E_{ox} - E_{red} + \Delta G_S \quad (2)$$

$$-\Delta G_S = \frac{e^2}{4\pi\epsilon_0}\left[\left(\frac{1}{2R^+} + \frac{1}{2R^-} - \frac{1}{R_{CC}}\right)\left(\frac{1}{\epsilon_s}\right) - \left(\frac{1}{2R^+} + \frac{1}{2R^-}\right)\left(\frac{1}{\epsilon_r}\right)\right] \quad (3)$$

where ΔE_{0-0} is the energy of the 0−0 transition of C_{60}, R^+ is the radii of the radical cation of BBA, and R^- is the radii of the radical anion of C_{60} (Table 1); e, ϵ_0, ϵ_s, and ϵ_r refer to elementary charge, vacuum permittivity, and static permittivities of the solvents used for rate measurements and redox potential measurements, respectively. The ΔG_{CS} and ΔG_{CR} values for C_{60}-spacer-BBA are summarized in Table 1. In a polar solvent such as PhCN and THF, charge separation via the excited singlet state of the C_{60} ($^1C_{60}$*) is exothermic and occurs easily, whereas in toluene, this process is endothermic and hardly occurs. The charge-separation process via the excited triplet state of the C_{60} ($^3C_{60}$*) is slightly exothermic in THF and PhCN.

Steady-State Absorption Measurements. Steady-state absorption spectra of BBA-spacer-C_{60} and its components in toluene are shown in Figure 4. The broad absorption bands at 640 and 710 nm of C_{60}-spacer-BBA are characteristic of the 58 conjugated π-electrons of the C_{60} moiety. The BBA moiety shows the absorption at shorter wavelength than 400 nm. For C_{60}-spacer-BBA, the absorption intensity in longer wavelength than 400 nm was almost the same as that of ref-C_{60}, indicating that no appreciable interaction in the ground state. From the MO calculation, the charge-transfer band would be anticipated in the longer wavelength region than 700 nm; however, the absorption intensity is too low to observe explicitly.

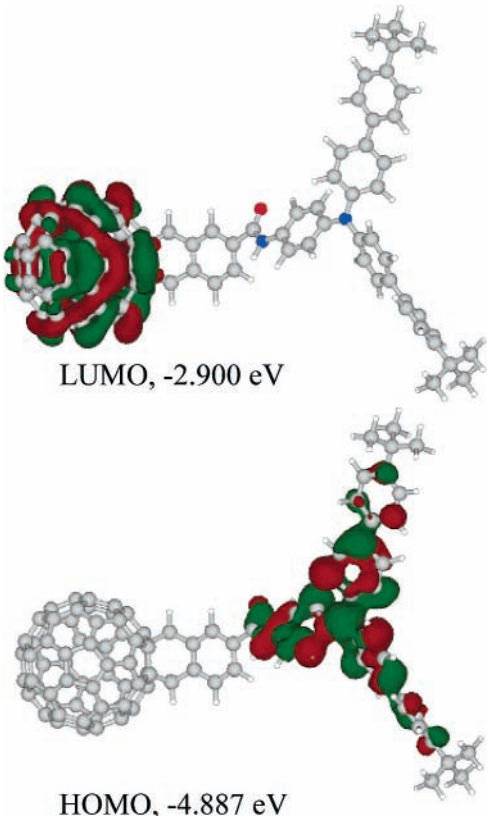

Figure 2. Optimized structures and electron distributions of LUMO and HOMO of C_{60}-spacer-BBA dyad calculated at B3LYP/3-21G level.

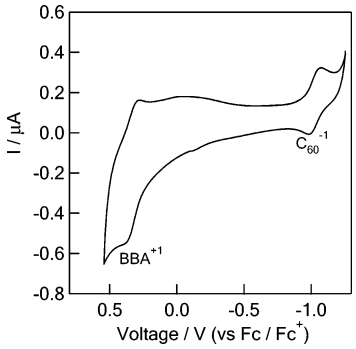

Figure 3. Cyclic voltammogram of C_{60}-spacer-BBA dyad (0.2 mM) in Ar-saturated PhCN containing Bu_4NClO_4 (0.05 M) as a supporting electrolyte at scan rate of 0.1 V s^{-1}.

TABLE 1: Free-Energy Changes for Charge Separation ($-\Delta G_{CS}$) and Charge Recombination ($-\Delta G_{CR}$) of C_{60}-Spacer-BBA

solvent	$-\Delta G^{S}_{CS}$/eV[a]	$-\Delta G^{T}_{CS}$/eV[a]	$-\Delta G_{CR}$/eV[a]
toluene	−0.20	−0.40	1.92
THF	0.27	0.07	1.45
PhCN	0.41	0.21	1.31

[a] Calculated from eqs 1−3 employing $\Delta E_{0-0} = 1.72$ eV for $^1C_{60}$*, $\Delta E_{0-0} = 1.52$ eV for $^3C_{60}$*, $E_{ox} = 0.33$ V for BBA, and $E_{red} = -1.02$ V for C_{60} vs Fc/Fc^+ in PhCN. $R^+ = 7.5$ Å for BBA, and $R^- = 4.0$ Å for C_{60}, and $R_{CC} = 15$ Å, as evaluated from Figure 2. Permittivities of toluene, THF, and PhCN are 2.38, 7.58, and 25.2, respectively.

Steady-State Fluorescence Measurements. Steady-state fluorescence spectrum of C_{60}-spacer-BBA in toluene exhibits the fluorescence peak (λ_f) at 720 nm as shown in Figure 5. Because the spectral shape of the fluorescence band of C_{60}-spacer-BBA is almost the same as that of ref-C_{60} in the same solvent (λ_f = 717 nm), the origin of the observed fluorescence of C_{60}-spacer-BBA is attributed to the C_{60} moiety. From the cross point of fluorescence band and absorption band after normalizing both intensities, the lowest excited singlet energy (E_{0-0}) of the C_{60} moiety was estimated to be 1.72 eV. The fluorescence intensity of C_{60}-spacer-BBA in toluene is almost the same as that of ref-C_{60}, when the absorbance at excitation wavelength was matched.

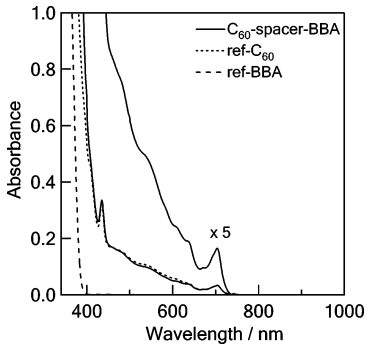

Figure 4. Steady-state absorption spectra of C_{60}-spacer-BBA (0.1 mM), ref-C_{60} (0.1 mM), and ref-BBA (0.1 mM) in toluene.

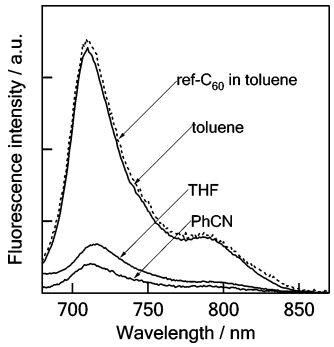

Figure 5. Steady-state fluorescence spectra of C_{60}-spacer-BBA (0.1 mM) in toluene, THF, and PhCN and ref-C_{60} in toluene; excitation at 500 nm, where the absorbance of both compounds was matched.

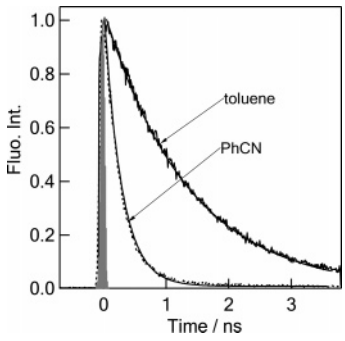

Figure 6. Fluorescence decay profiles around 710−730 nm of C_{60}-spacer-BBA dyad (0.1 mM) in toluene and PhCN after 410 nm laser irradiation. Filled curve indicates laser profile. Solid lines are fitting curves.

In polar solvents such as THF and PhCN, the fluorescence intensity of C_{60}-spacer-BBA becomes lower than that in toluene, as shown in Figure 5. Such a decrease in fluorescence intensity of the C_{60}-spacer-BBA in polar solvent suggests the electron transfer via the $^1C_{60}$* moiety.

Fluorescence Lifetimes. The time profiles of the fluorescence intensity at the peak position of the $^1C_{60}$* moiety in C_{60}-spacer-BBA in toluene and PhCN are shown in Figure 6. In toluene, the fluorescence decay of the $^1C_{60}$* moiety obeys a single-exponential function, yielding the fluorescence lifetime of 1400 ps, which is the same as that of ref-C_{60}.[17a] This finding indicates that both energy and electron transfers do not take place for

TABLE 2: Fluorescence Lifetime (τ_f at 710−730 nm), Charge-Separation Rate Constant via $^1C_{60}$* (k^S_{CS}), Quantum Yield for Charge Separation (Φ^S_{CS}) via $^1C_{60}$*, Charge-Recombination Rate Constant (k_{CR}) of C_{60}-Spacer-BBA at Room Temperature

solvent	τ_f/ps	k^S_{CS}/s^{-1}	Φ^S_{CS}	k^T_{CS}/s^{-1} [a]	k_{CR}/s^{-1}	τ_{RIP}/ns
toluene	1400		0.00			
THF	340	2.2×10^9	0.76	3.4×10^7	2.8×10^6	360
PhCN	270	3.0×10^9	0.81	4.2×10^7	3.1×10^6	330

[a] The k^T_{CS} (charge separation rate constant via $^3C_{60}$*) values at −10 °C.

C_{60}-spacer-BBA in toluene. In PhCN, the fluorescence intensity of the $^1C_{60}$* moiety in C_{60}-spacer-BBA shows fast decay obeying a single-exponential kinetics, giving a short fluorescence lifetime (τ_f = 370 ps). In THF, τ_f = 340 ps was similarly evaluated as listed in Table 2.

The difference between the τ_f values evaluated from the main decays in 710−730 nm in polar and nonpolar solvents can be attributed predominantly to charge separation via the $^1C_{60}$* moiety in C_{60}-spacer-BBA, generating the radical ion-pair state ($C_{60}^{\bullet-}$-spacer-$BBA^{\bullet+}$) in polar solvents.

From the τ_f value of the $^1C_{60}$* moiety in C_{60}-spacer-BBA, the intramolecular charge-separation rate constant (k^S_{CS}) in THF and PhCN was evaluated, as summarized in Table 2 using

$$k^S_{CS} = (1/\tau_f)_{sample} - (1/\tau_f)_{ref} \quad (4)$$

where $(\tau_f)_{ref}$ is the fluorescence lifetime of ref-C_{60} in toluene.[17e] Thus, the k^S_{CS} values were evaluated to be $(2.2-3.0) \times 10^9$ s^{-1} in polar solvents, which indicate that charge separation via the $^1C_{60}$* moiety is an effective process in polar solvents. The quantum yields of charge separation (Φ^S_{CS}) via the $^1C_{60}$* moiety in the C_{60}-spacer-BBA in polar solvents were evaluated from

$$\Phi^S_{CS} = [(1/\tau_f)_{sample} - (1/\tau_f)_{ref}]/(1/\tau)_{sample} \quad (5)$$

Thus, Φ^S_{CS} = 0.76 and 0.81 were calculated for the C_{60}-spacer-BBA in THF and PhCN, respectively, which indicates that charge separation via the $^1C_{60}$* moiety is competitive with the intersystem crossing (ISC) process to the $^3C_{60}$* moiety even in PhCN.

Thus, the k^S_{CS} and Φ^S_{CS} values for C_{60}-spacer-BBA are smaller than those reported for C_{60}−BBA with short linkage,[26] indicating that the long distance between the donor and acceptor for C_{60}-spacer-BBA is disadvantageous for the charge-separation system in polar solvents.

Nanosecond Transient Absorption Measurements. Transient absorption spectra observed by the nanosecond laser excitation (532 nm) of C_{60}-spacer-BBA in PhCN are shown in Figure 7. The broad absorption bands were observed in the region of 600−1200 nm, which are the overlapping regions of the absorption bands of $BBA^{\bullet+}$ (880 nm)[26] and $C_{60}^{\bullet-}$ (1000 nm).[17e] From the decay time profile at 880 nm, the charge-recombination rate constant (k_{CR}) was evaluated to be 3.1×10^6 s^{-1}, from which the lifetime (τ_{RIP}) of the charge-separated state was calculated to be 320 ns at room temperature.

In THF, similar transient spectra to those in PhCN were observed (Supporting Information; Figure S2), showing the generation of the charge-separated state, which persists with τ_{RIP} = 360 ns.

In toluene, transient absorption band was observed around 700 nm at 100 ns (Figure 8). The possible species of the absorption band is the $^3C_{60}$* moiety (700 nm), [11b] which did not show the appreciable decay during 1 μs, because of its long lifetime more than 40 μs.[17e] This observation was supported by the positive ΔG^S_{CS} value in toluene (Table 1), suggesting difficulty of charge separation.

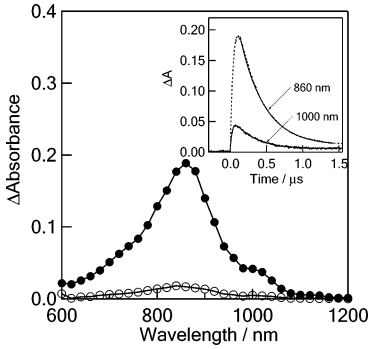

Figure 7. Nanosecond transient absorption spectra of C_{60}-spacer-BBA dyad (0.1 mM) observed by 532 nm laser irradiation in at 0.1 μs (●) and 1.0 μs (○) in PhCN at room temperature. Inset: absorption−time profiles at 860 and 1000 nm in PhCN.

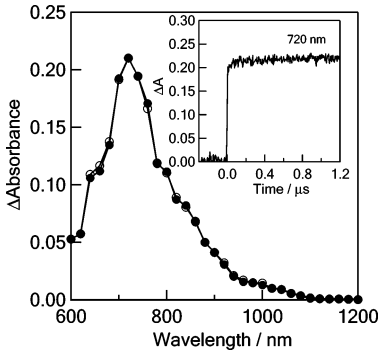

Figure 8. Nanosecond transient absorption spectra of C_{60}-spacer-BBA dyad (0.1 mM) observed by 532 nm laser irradiation in at 0.1 μs (●) and 1.0 μs (○) in toluene at room temperature. Inset: absorption−time profiles at 720 nm in toluene.

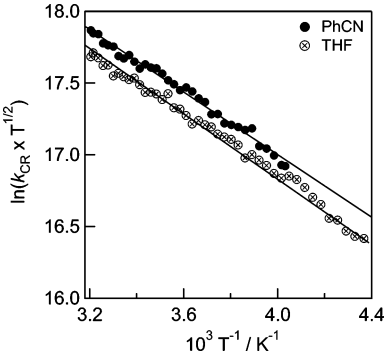

Figure 9. Semiclassical Marcus (modified Arrhenius) plots of the temperature dependence of k_{CR} for C_{60}-spacer-BBA in PhCN and THF.

Temperature Effect. The energy barriers for the charge-separation and charge-recombination processes can be estimated by measuring the temperature dependence of the k^S_{CS} and k_{CR} values. From the semiclassical Marcus equation,[27] the electron-transfer rate constant (k) can be described as follows:

$$\ln(k\sqrt{T}) = \ln\left(\frac{2\pi^{3/2}|V|^2}{h\sqrt{\lambda k_B}}\right) - \frac{\Delta G^{\ddagger}}{k_B T} \quad (6)$$

where T, $|V|$, h, λ, k_B, and $\Delta G^{\ddagger}$ are absolute temperature, the electron coupling matrix element, Planck's constant, the reorganization energy, Boltzman's constant, and Gibb's activation energy in the Marcus theory,[27] respectively. Figure 9 shows the modified Arrhenius plot for the semiclassical Marcus eq 6,[27]

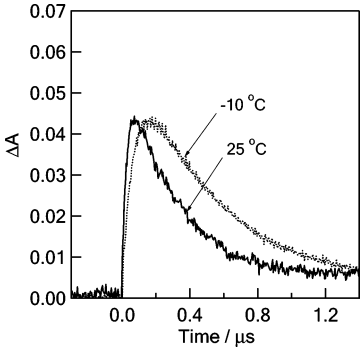

Figure 10. Nanosecond transient absorption spectra of C_{60}-spacer-BBA dyad (0.1 mM) observed by 532 nm laser irradiation in at 0.1 μs (●) and 1.0 μs (○) in PhCN at low temperature (−10 °C). Inset: absorption−time profiles at 860 and 1000 nm in PhCN.

TABLE 3: Gibbs Activation Energy ($\Delta G^{\ddagger}_{CR}$), Reorganization Energy (λ_{CR}), and Electron Coupling Matrix Element ($|V_{CR}|$) for Charge-Recombination Process of $C_{60}^{\bullet-}$-Spacer-BBA$^{\bullet+}$ in THF and PhCN

solvent	$\Delta G^{\ddagger}_{CR}$/eV	λ_{CR}/eV	$\lvert V_{CR}\rvert$/cm^{-1}
THF	0.10	0.87	0.64
PhCN	0.09	0.77	0.60

TABLE 4: Gibbs Activation Energy ($\Delta G^{\ddagger}_{CS}$), Reorganization Energy (λ_{CS}), and Electron Coupling Matrix Element ($|V_{CS}|$) for Charge-Separation Process of C_{60}-Spacer-BBA in PhCN

CS process	$\Delta G^{\ddagger}_{CS}$/eV	λ_{CS}/eV	$\lvert V_{CS}\rvert$/cm^{-1}
via $^1C_{60}$*	0.09	0.17	12.9
via $^3C_{60}$*	0.11	0.05	1.61

which shows a linear relation between $\ln(k_{CR}T^{1/2})$ values and $1/T$. The observed changes in k_{CR} value in the temperature region shown in Figure 9 were larger than the experimental error (±5%; Supporting Information, Figure S3). From the slope, i.e., $(-\Delta G^{\ddagger}_{CR}/k_B)$, the $\Delta G^{\ddagger}_{CR}$ value was estimated to be 0.098 and 0.094 eV in THF and PhCN, respectively. The λ values for the charge-recombination process (λ_{CR}) were calculated to be 0.87 and 0.77 eV in THF and PhCN,[32] respectively, from the following relation:[27]

$$\Delta G^{\ddagger} = \frac{(\Delta G_{CR} + \lambda)^2}{4\lambda} \qquad (7)$$

From the comparison of the λ_{CR} values with the ΔG_{CR} values in PhCN and THF (−1.31 and −1.45 eV, respectively), the charge-recombination processes are considered to take place in the Marcus inverted region.[27] This clearly explains the longer lifetimes of $C_{60}^{\bullet-}$-spacer-BBA$^{\bullet+}$ compared with those of other dyads.[5] The $|V_{CR}|$ values in PhCN and THF were calculated to be 0.60 and 0.64 cm^{-1}, respectively, from the intercept of the slope in Figure 9. These small $|V_{CR}|$ values are reasonable to explain the slow charge recombination of $C_{60}^{\bullet-}$-spacer-BBA$^{\bullet+}$ in polar solvents. From the temperature dependency of fluorescence temporal profiles (Supporting Information; Figure S4), the $\Delta G^{\ddagger S}_{CS}$ value in PhCN was evaluated to be 0.09 eV, giving $\lambda^{S}_{CS} = 0.17$ eV and $|V^{S}_{CS}| = 12.9$ cm^{-1}. Compared with $\Delta G^{S}_{CS} = -0.41$ eV, the charge-separation processes via $^1C_{60}$* moiety are also considered to take place in the Marcus inverted region.[33] Indeed, the k^{S}_{CS} values are moderate in the range of (2.2−3.0) × 10^9 s^{-1} at room temperature. On lowering the temperature, the rise of the radical ions seems to become slowed, as shown in Figure 10 for $C_{60}^{\bullet-}$-spacer-BBA$^{\bullet+}$ in PhCN at −10 °C, suggesting the charge separation also takes place via the $^3C_{60}$* moiety. From the rise time profile of the $C_{60}^{\bullet-}$ moiety, the rate constant (k^{T}_{CS}) for the charge separation can be evaluated to be 4.2×10^7 s^{-1} at −10 °C. In PhCN, the ΔG^{T}_{CS} value is negative allowing the charge separation via $^3C_{60}$*. In THF, similar phenomena were observed giving $k^{T}_{CS} = 3.4 \times 10^7$ s^{-1} at −10 °C, because the ΔG^{T}_{CS} value is slightly negative. Probably, $C_{60}^{\bullet-}$-spacer-BBA$^{\bullet+}$ may be stabilized in these polar solvents by lowering temperature, increasing the ΔG^{T}_{CS} value negatively.

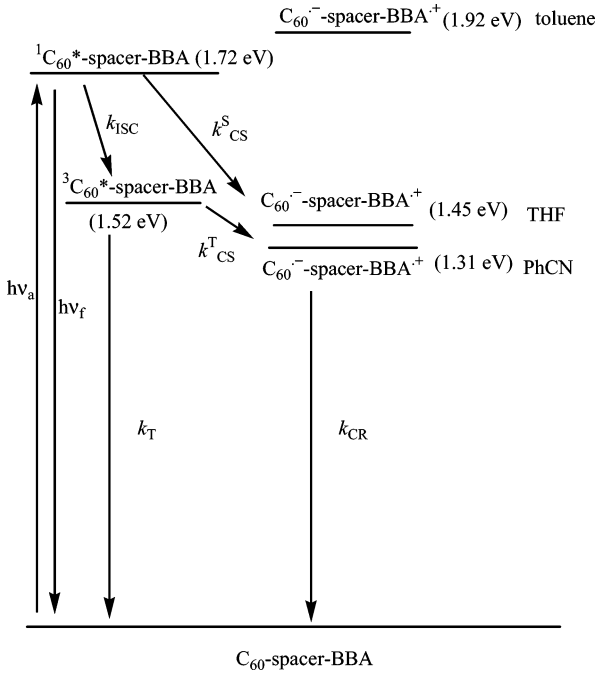

Figure 11. Schematic energy diagram for electron-transfer processes of C_{60}-spacer-BBA in toluene, THF, and PhCN.

From the temperature dependency of the rise temporal profiles of the $C_{60}^{\bullet-}$ moiety, the $\Delta G^{\ddagger T}_{CS}$ value in PhCN was evaluated to be 0.11 eV, from which $\lambda^{T}_{CS} = 0.05$ eV and $|V^{T}_{CS}| = 1.61$ cm^{-1}. From $\Delta G^{\ddagger T}_{CS} = -0.11$ eV, the charge-separation processes via the $^3C_{60}$* moiety are considered to take place at almost the top region of the Marcus parabola.[27] Indeed, the k^{T}_{CS} values are slow at −10 °C.

Energy Diagram. Figure 11 shows an energy diagram of C_{60}-spacer-BBA when the 532 nm laser light is used as the excitation light. Energy levels of the radical ion-pairs were cited from Table 1. In THF and PhCN, the charge separation takes place via $^1C_{60}$*-spacer-BBA, as indicated by the weak fluorescence intensity and short fluorescence lifetime, because the energy levels of $C_{60}^{\bullet-}$-spacer-BBA$^{\bullet+}$ were lower than those for $^1C_{60}$*-spacer-BBA. In toluene, on the other hand, charge separation is impossible via $^1C_{60}$*, only generating $^3C_{60}$* via the ISC process. Thus, the generation of $^3C_{60}$*-spacer-BBA with the ISC process from $^1C_{60}$*-spacer-BBA is also possible, because the Φ^{S}_{CS} values are less than unity in polar solvents. The charge separation via $^3C_{60}$*-spacer-BBA becomes prominent at low temperature, probably because solvation of $C_{60}^{\bullet-}$-spacer-BBA$^{\bullet+}$ increased its stabilization.

Comparison with Other Systems. For C_{60}−BBA with short linkage (10 Å), the k^{S}_{CS} values ((3.4−5.0) × 10^{10} s^{-1}) are 1 order larger than those for C_{60}-spacer-BBA; the Φ^{S}_{CS} values (0.95−0.99) are also larger than those for C_{60}-spacer-BBA. These observations indicate the charge separation is effective with short linkage. The lifetime of $C_{60}^{\bullet-}$-spacer-BBA$^{\bullet+}$ was evaluated to be 330 ns in PhCN, which is slightly longer than that of $C_{60}^{\bullet-}$-BBA$^{\bullet+}$ (220 ns in PhCN at room temperature),[26] probably because of the smaller $|V_{CR}|$ values, which are usually

inverted proportional to the distance between the electron and the hole connected by covalent bonds.

Compared with aromatic amine donors such as dimethylaniline and diphenylaniline, the BBA moiety has excellent donor ability, giving persistent radical ion-pair, irrespective the distance between the amine and C_{60} moieties. For example, for NMPC_{60}-TPA dyad, the τ_{RIP} value was less than 10 ns.[34] In the case of a triad composed of NMPC_{60}-quterthiophene-TPA, the τ_{RIP} value was evaluated to be 18 ns in DMF at room temperature.[35b] The τ_{RIP} value for a triad composed of the C_{60}-fluorene-diphenylamine was evaluated to be 150 ns in DMF at room temperature.[35a] In the case of C_{60}-bridge-dimethylaniline systems, the τ_{RIP} values in the range of 8−250 ns were reported, depending on the kinds and lengths of the bridge molecules.[5a,5b] Compared with these C_{60} and amine systems, $C_{60}^{\bullet-}$-spacer-BBA$^{\bullet+}$ showed long τ_{RIP} value.

Summary

For C_{60}-spacer-BBA, the photoinduced charge separation via $^1C_{60}$*-spacer-BBA was observed in polar solvents at room temperature. By lowering the temperature, the contribution of charge separation via $^3C_{60}$*-spacer-BBA increased. The lifetimes of 320−360 ns were evaluated for the $C_{60}^{\bullet-}$-spacer-BBA$^{\bullet+}$ in PhCN and THF, respectively, at room temperature. Furthermore, it is revealed that a smaller λ_{CR} value than the absolute values of ΔG_{CR} leads to the inverted region of the Marcus parabola, resulting in slow the charge-recombination rate. The $C_{60}^{\bullet-}$-spacer-BBA$^{\bullet+}$ gains a chance to mix with the $^3C_{60}$*-spacer-BBA, which makes the lifetime of $C_{60}^{\bullet-}$-spacer-BBA$^{\bullet+}$ long. With an increase of distance between donor and acceptor from 10 to 15 Å, the lifetimes increase slightly. These findings afford a guideline to design new dyads.

Experimental Section

Materials. [60]Fullerene (C_{60}) was obtained from MER Corporation, USA (99.5% purity). PhCN, toluene, *n*-hexane, benzene-d_6, *N*-methylglycine, and α-cyano-4-hydroxycinnamic acid were purchased from Aldrich Chemicals (Milwaukee, WI).

Synthesis of 3. A mixture of 4-nitroaniline (310 mg, 2.24 mmol), 4-*tert*-butyl-4′-iodobiphenyl (3.02 g, 4.49 mmol), Cu powder (856 mg, 13.4 mmol), K_2CO_3 (3.70 g, 26.8 mmol), and 18-crown-6 (650 mg, 2.46 mmol) in 1,2,4-trichlorobenzene (30 mL) was heated at 165 °C under Ar atmosphere for 24 h. The reaction mixture was filtered, and the filtrate was passed over a short column on SiO_2. Elution with hexane removed 1,2,4-trichlorobenzene followed by elution with $CHCl_3$−hexane (ca. 1/1) to afford the crude product. Further purification by SiO_2 column chromatography (eluent: $CHCl_3$/hexane (1/4)) afforded **3** as a bright orange crystal (1.05 g, 84% yield). ^{1}H NMR ($CDCl_3$, 500 MHz): δ 8.08−8.07 (2H, m, Ar−H), 7.59−7.58 (4H, m, Ar−H), 7.54−7.52 (4H, m, Ar−H), 7.48−7.46 (4H, m, Ar−H), 7.27−7.19 (4H, m, Ar−H), 7.05−7.03 (2H, m, Ar−H), 1.37 (18H, s, *tert*-Bu).

Synthesis of 4. A mixture of **3** (600 mg, 1.08 mmol) and 5% Pd−C (131 mg) in THF (40 mL) was stirred under H_2 atmosphere at room temperature for 24 h. The reaction mixture was filtered, and the filtrate was evaporated. The residue was purified by SiO_2 column chromatography (eluent: $CHCl_3$/hexane (1/3)) to afford amine **4** (520 mg, 92%) as a bright red-brown crystal.

^{1}H NMR ($CDCl_3$, 270 MHz): δ 7.51−7.49 (m, 4H, Ar−H), 7.45−7.42 (m, 8H, Ar−H), 7.13 (d, 4H, Ar−H, J = 8.5 Hz), 7.05 (d, 2H, Ar−H, J = 8.5 Hz), 6.69 (d, 2H, Ar−H, J = 8.5 Hz), 1.36 (s, 18H, *tert*−Bu).

Synthesis of 6. To a solution of **4** (500 mg, 0.95 mmol) and Et_3N (0.18 mL, 1.28 mmol) in THF (30 mL) was added dropwise a solution of **5** (320 mg, 0.98 mmol) in THF (20 mL) at 0 °C. After being stirred at 0 °C for 1 h, the reaction mixture was stirred at room temperature for 3 h. Then the reaction mixture was diluted with 70 mL of $CHCl_3$ and washed with 1 M HCl (2 × 10 mL), brine (20 mL), and water (20 mL). Evaporation of the solvent gave the crude product, which was purified by preparative HPLC to give **5** as a bright green solid (440 mg, 57%). ^{1}H NMR ($CDCl_3$, 500 MHz): δ 7.89 (bs, 1H, NH), 7.79−7.77 (m, 2H, Ar−H), 7.56−7.44 (m, 15H, Ar−H), 7.20−7.16 (m, 6H, Ar−H), 4.80−4.79 (m, 2H, CH_2Br), 4.69−4.68 (m, 2H, CH_2Br), 1.36 (s, 18H, *tert*-Bu).

Synthesis of C_{60}-spacer-BBA. A mixture of **6** (60 mg, 0.074 mmol), KI (87 mg, 0.52 mmol), 18-crown-6 (79 mg, 0.30 mmol), and C_{60} (69 mg, 0.096 mmol) in dry toluene (25 mL) was refluxed for 16 h under argon atmosphere. The reaction mixture was evaporated to dryness, and the residue was subjected to silica gel column chromatography (from 50% toluene in $CHCl_3$ to 100% $CHCl_3$) to afford the crude product (96 mg). The crude product was subjected to preparative HPLC to afford C_{60}-spacer-BBA (22 mg, 22%). Mp: >300°C. ^{1}H NMR ($CDCl_3$, 500 MHz): δ 7.89 (bs, 1H, NH), 7.79−7.77 (m, 2H, Ar−H), 7.56−7.44 (m, 15H, Ar−H), 7.20−7.16 (m, 6H, Ar−H) 4.80−4.79 (bs, 2H, CH_2), 4.69−4.68 (bs, 2H, CH_2), 1.36 (s, 18H, *tert*-Bu). ^{13}C NMR ($CDCl_3$, 125 MHz): δ 165.41, 156.28, 155.94, 149.68, 147.60, 146.46, 146.39, 146.16, 145.36, 144.83, 144.59, 144.57, 144.15, 143.06, 142.50, 142.10, 142.03, 141.49, 140.14, 138.81, 137.57, 135.14, 134.63, 133.05, 128.33, 127.61, 126.60, 126.22, 125.60, 125.15, 123.87, 121.64, 65.63, 65.59, 45.06, 34.57, 31.45, 29.77. FT-IR (KBr): ν 3433 (N−H), 1652 (CO−NH), 1493, 1261, 1098, 1020 cm^{-1}. Calcd for $(C_{107}H_{46}N_2O)(CHCl_3)_{0.5}(H_{20})_{4.0}$: C, 85.65; H, 3.65; N, 1.86%. Found: C, 85.86; H, 3.79; N, 1.88.

Synthesis of ref-BBA. To a solution of **4** (27.8 mg, 53.0 μmol) and triethylamine (8.00 μL, 57.4 μmol) in chloroform (1.00 mL) was added acetyl chloride (5.00 μL, 70.3 μmol) at 0 °C. The mixture was stirred at room temperature overnight. The reaction mixture was evaporated to dryness, and the residue was subjected to silica gel column chromatography (chloroform/ethyl acetate = 19/1, R_f = 0.22) to afford the crude product (28.1 mg). The crude product was subjected to preparative HPLC to afford ref-BBA as a white solid (22.4 mg, 40.0 μmol, 75%). Mp: 146−150 °C. ^{1}H NMR ($CDCl_3$, 400 MHz): δ 7.63 (s, 1H), 7.52−7.39 (m, 16H), 6.85 (br s, 4H), 2.24 (s, 3H), 1.35 (s, 18H) ppm. IR (KBr): 2961, 1655, 1601, 1508, 1497, 1319, 1273, 820, 527 cm^{-1}. FAB-MS (matrix: mNBA): *m*/*z* 566 [M]$^+$. Anal. Calcd for $C_{40}H_{42}N_2O$: C, 84.77; H, 7.47; N, 4.94. Found: C, 84.33; H, 7.74; N, 5.14.

Measurements

Electrochemical Measurements. Reduction potentials (E_{red}) and oxidation potentials (E_{ox}) were measured by a cyclic voltammetry with a potentiostat (BAS CV50W) in a conventional three electrode-cell equipped with Pt-working and counter electrodes with an Ag/Ag$^+$ reference electrode at scan rate of 100 mV/s. The E_{red} and E_{ox} were expressed vs ferrocene/ferrocenium (Fc/Fc$^+$) used as internal reference. In each case, a solution containing 0.2 mM of a sample with 0.05 M of *n*-Bu_4NClO_4 (Fluka purest quality) was deaerated with argon bubbling before measurements.

Steady-State Measurements. Steady-state absorption spectra in the visible and near-IR regions were measured on a Jasco V570 DS spectrophotometer. Steady-state fluorescence spectra

were measured on a Shimadzu RF-5300 PC spectrofluorophotometer equipped with a photomultiplier tube having high sensitivity in the 700−800 nm region.

Time-Resolved Fluorescence Measurements. The time-resolved fluorescence spectra were measured by single photon counting method using a streakscope (Hamamatsu Photonics, C4334−01) as a detector and the laser light (second harmonic generation (SHG), 410 nm) of a Ti:sapphire laser (Spectra-Physics, Tsunami 3950-L2S, 1.5 ps fwhm) as an excitation source.[36] Lifetimes were evaluated with software attached to the equipment.

Nanosecond Transient Absorption Measurements. Nanosecond transient absorption measurements were carried out using SHG (532 nm) of a Nd:YAG laser (Spectra-Physics, Quanta-Ray GCR-130, 5 ns fwhm) as an excitation source. For transient absorption spectra in the near-IR region (600−1200 nm) and the time profiles, monitoring light from a pulsed Xe lamp was detected with a Ge-APD (Hamamatsu Photonics, B2834). For the measurements in the visible region (400−1000 nm), a Si−PIN photodiode (Hamamatsu Photonics, S1722−02) was used as a detector.[17,36]

Molecular Orbital Calculations. The optimized structure, energy levels of the molecular orbitals, and electron densities were calculated by *GAUSSIAN 98* (B3LYP/3-21G level).[30]

Acknowledgment. This present work was supported by a Grants-in-Aid on Scientific Research on Priority Areas (417) from the Ministry of Education, Culture, Sports, Science and Technology of Japan.

Supporting Information Available: Space-filled molecular structure, nanosecond transient spectra in THF, and time profiles with changing temperature in THF, semiclassical Marcus plots. This material is available free of charge via the Internet at http://pubs.acs.org.

References and Notes

(1) Foote, C. S. In *Topics in Current Chemistry; Photophysical and Photochemical Properties of Fullerenes*; Matty, J., Ed.; Springer-Verlag: Berlin, 1994; Series 169, p 347.

(2) *Fullerene, Chemistry, Physics and Technology*; Kadish, K. M., Ruoff, R. S., Eds.; Wiley-Interscience: New York, 2000.

(3) Ramamurthy, V.; Schanze, K. S. *Molecular and Supramolecular Photochemistry*; Marcel Dekker: New York, 2001; Vol.7.

(4) (a) Liddell, P. A.; Sumida, J. P.; Macpherson, A. N.; Noss, L.; Seely, G. R.; Clark, K. N.; Moore, A. L.; Moore, T. A.; Gust, D. *Photochem. Photobiol.* **1994**, *60*, 537. (b) Imahori, H.; Cardoso, S.; Tatman, D.; Lin, S.; Noss, L.; Seely, G. R.; Sereno, L.; Silber, C.; Moore, T. A.; Moore, A. L.; Gust, D. *Photochem. Photobiol.* **1995**, *62*, 1009. (c) Kuciauskas, D.; Lin, S.; Seely, G. R.; Moore, A. L.; Moore, T. A.; Gust, D.; Drovetskaya, T.; Reed, C. A.; Boyd, P. D. W. *J. Phys. Chem.* **1996**, *100*, 15926.

(5) (a) Williams, R. M.; Zwier, M. N.; Verhoeven, J. W. *J. Am. Chem. Soc.* **1995**, *117*, 4093. (b) Williams, R. M.; Koeberg, M.; Lawson, J. M.; An, Y.-Z.; Rubin, Y.; Paddon-Row: M. N.; Verhoeven, *J. Org. Chem.* **1996**, *61*, 5055. (c) Thomas, K. G.; Biju, V.; George, M. V.; Guldi, D. M.; Kamat, P. V. *J. Phys. Chem. A* **1998**, *102*, 5341. (d) Thomas, K. G.; Biju, V.; Guldi, D. M.; Kamat, P. V.; George, M. V. *J. Phys. Chem. B* **1999**, *103*, 8864. (e) Thomas, K. G.; Biju, V.; Guldi, D. M.; Kamat, P. V.; George, M. V. *J. Phys. Chem. A* **1999**, *103*, 10755.

(6) Sariciftci, N. S.; Wudl, F.; Heeger, A. J.; Maggini, M.; Scorrano, G.; Prato, M.; Bourassa, J.; Ford, P. C. *Chem. Phys. Lett.* **1995**, *247*, 510.

(7) (a) Imahori, H.; Hagiwara, K.; Aoki, M.; Akiyama, T.; Taniguchi, S.; Okada, T.; Shirakawa, M.; Sakata, Y. *J. Am. Chem. Soc.* **1996**, *118*, 11771. (b) Imahori, H.; Ozawa, S.; Uchida, K.; Takahashi, M.; Azuma, T.; Ajavakom, A.; Akiyama, T.; Hasegawa, M.; Taniguchi, S.; Okada, T.; Sakata, Y. *Bull. Chem. Soc. Jpn.* **1999**, *72*, 485. (c) Imahori H.; Tamaki K.; Guldi D M.; Luo C.; Fujitsuka M.; Ito O.; Sakata Y.; Fukuzumi *J. Am. Chem. Soc*. **2001**, *123*, 2607.

(8) (a) Samanta, A.; Kamat, P. V. *Chem. Phys. Lett.* **1992**, *199*, 635. (b) Guldi, D. M.; Maggini, M.; Scorrano, G.; Prato, M. *J. Am. Chem. Soc.* **1997**, *119*, 974. (c) Guldi, D. M.; Maggini, M.; Scorrano, G.; Prato. M. *Res. Chem. Intermed.* **1997**, *23*, 561. (d) Thomas, K. G.; Biju, V.; George, M. V.; Guldi, D. M.; Kamat, P. V. *J. Phys. Chem. A* **1998,** *102*, 5341. (e) Guldi, D. M.; Garscia, G. T.; Mattay, J. *J. Phys. Chem. A* **1998**, *102*, 9679. (f) Maggini, M.; Guldi, D. M.; Mondini, S.; Scorrano, G.; Paolucci, F.; Ceroni, P.; Roffia, S. *Chem. Eur. J.* **1998**, *4*, 1992. (g) Polese, A.; Mondini, S.; Bianco, A.; Toniolo, C.; Scorrano, G.; Guldi, D. M.; Maggini, M. *J. Am. Chem. Soc.* **1999**, *121*, 3446.

(9) Llacay, J.; Veciana, J.; Vidal-Gancedo, J.; Bourdelnde, J. L.; Gonzalez-Moreno, R.; Rovia, C. *J. Org. Chem.* **1998**, *63*, 5201.

(10) Tkachenko, N. V.; Rantala, L.; Tauber, A. Y.; Helaja, J.; Hynninen, P. V.; Lemmetyinen, H. *J. Am. Chem. Soc.* **1999**, *121*, 9378.

(11) Schuster, D. I.; Cheng, P.; Wilson, S. R.; Prokhorenko, V.; Katterle, M.; Holzwarth, A. R.; Braslavsky, S. E.; Klihm, G.; Williams, R. M.; Luo, C. *J. Am. Chem. Soc.* **1999**, *121*, 11599.

(12) (a) Yamashiro, T.; Aso, Y.; Otsubo, T.; Tang, H.; Harima, T.; Yamashita, K. *Chem. Lett.* **1999**, 443. (b) Fujitsuka, M.; Ito, O.; Yamashiro, T.; Aso, Y.; Otsubo, T. *J. Phys. Chem. A* **2000**, *104*, 4876. (c) van Hal, P. A.; Knol, J.; Langeveld-Voss, B. M. W.; Meskers, S. C. J.; Hummelen, J. C.; Janssen, R. A. J. *J. Phys. Chem. A* **2000**, *104*, 5974. (d) Apperloo, J. J.; Langeveld-Voss, B. M. W.; Knol, J.; Hummelen, J. C.; Janssen, R. A. J. *Adv. Mater.* **2000**, *12*, 908. (e) Fujitsuka, M.; Matsumoto, K.; Ito, O.; Yamashiro, T.; Aso, Y.; Otsubo, T. *Res. Chem. Intermed*. **2001**, *27*, 73. (f) Fujitsuka, M.; Masuhara, A.; Kasai, H.; Oikawa, H.; Nakanishi, H.; Ito, O.; Yamashiro, T.; Aso, Y.; Otsubo, T. *J. Phys. Chem. B* **2001**, *105*, 9930. (g) van Hal, P. A.; Beckers, E. H. A.; Meskers, S. C. J.; Janssen, R. A. J.; Jousselme, B.; Blanchard, P.; Roncali, J. *Chem.-Eur. J.* **2002**, *8*, 5415. (h) Beckers, E. H. A.; van Hal, P. A.; Dhanabalan, A.; Meskers, S. C. J.; Knol, J.; Hummelen, J. C.; Janssen, R. A. J. *J. Phys. Chem. A* **2003**, *107*, 6218.

(13) (a) Arbogast, J. W.; Foote, C. S.; Kao, M. *J. Am. Chem. Soc.* **1192**, *114*, 2277. (b) Foote, C. S. *Top. Curr. Chem.*, **1994**, *169*, 347.

(14) Wang, Y. *J. Phys. Chem.* **1992**, *96*, 764.

(15) (a) Seshadri, R.; Rao, C. N. R.; Pal, H.; Mukherjee, T.; Mittal, J. P. *Chem. Phys. Lett.* **1993**, *205*, 395. (b) Ghosh, H. N.; Pal, H.; Saper, A. V.; Mittal, J. P. *J. Am. Chem. Soc.* **1993**, *115*, 11722.

(16) Schaffner, E.; Fischer, H. *J. Phys. Chem.* **1993**, *97*, 13149.

(17) (a) Watanabe, A.; Ito, O. *J. Phys. Chem.* **1994**, *98*, 7736. (b) Ito, O.; Sasaki, Y.; Yoshikawa, Y.; Watanabe, A. *J. Phys. Chem.* **1995**, *99*, 9838. (c) Sasaki, Y.; Yoshikawa, Y.; Watanabe, A.; Ito, O. *J. Chem. Soc., Faraday Trans.* **1995**, *91*, 2287. (d) Alam, M. M.; Watanabe, A.; Ito, O. *J. Photochem. Photobiol. A* **1997**, *104*, 59. (e) Luo, C.; Fujitsuka, M.; Watanabe, A.; Ito, O.; Gan, L.; Huang, Y.; Huang, C. H. *J. Chem. Soc., Faraday Trans.* **1998**, *94*, 527.

(18) (a) Bennati, M.; Grupp, A.; Bäuerle, P.; Mehring, M. *Chem. Phys.* **1994**, *185*, 221. (b) Bennati, M.; Grupp, A.; Bäuerle, P.; Mehring, M. *Mol. Cryst. Liq. Cryst.* **1994**, *256*, 751.

(19) (a) Ma, B.; Laeson, G. E.; Bunker, C. E.; Kitaygorodskiy, A.; Sun, Y.-P. *Chem. Phys. Lett.* **1995**, *247*, 51. (b) Sun, Y.-P.; Ma, B.; Lawson, G. E. *Chem. Phys. Lett.* **1995**, *233*, 57. (c) Lawson, G. E.; Kitaygorodskiy, A.; Ma, B.; Bunker, C. E.; Sun, Y.-P. *J. Chem. Soc., Chem. Commun.* **1995**, 2225.

(20) Fukuzumi, S.; Suenobu, T.; Patz, M.; Hirasaka, T.; Itoh, S.; Fujitsuka, M.; Ito, O. *J. Am. Chem. Soc.* **1998**, *120*, 8060.

(21) (a) Martín, N.; Sánchez, L.; Seoane, C.; Andreu, R.; Garín, J.; Orduna, J. *Tetrahedron Lett.* **1996**, *37*, 5979. (b) Martín, N.; Sánchez, L.; Guldi, D. M. *Chem. Commun*. **2000**, 113. (c) Martín, N.; Pérez, I.; Sánchez, L.; Seoane, C. *J. Org. Chem*. **1997**, *62*, 5690. (d) Herranz, M. A.; Martín, N. *Org. Lett.* **1999**, *1*, *2005*. (e) Martín, N.; Sanchez, L.; Herranz, M. A.; Guldi, D. M. *J. Phys. Chem. A* **2000**, *104*, 4648. (f) Herranz, M. A.; Martín, N.; Sánchez, L.; Seoane, C.; Guldi, D. M. *J. Organomet. Chem.* **2000**, *599*, 2. (g) Guldi, D. M.; González, S.; Martín, N.; Antón, A.; Garín, J. Orduna, J. *J. Org. Chem.* **2000**, *65*, 1978. (h) Herranz, M. A.; Illescas, B.; Martín, N.; Luo, C.; Guldi, D. M. *J. Org. Chem*. **2000**, *65*, 5728. (i) González, S.; Martín, N.; Swartz, A.; Guldi, D. M. *Org. Lett*. **2003**, *5*, 557.

(22) (a) Imahori, H.; Hagiwara, K.; Akiyama, T.; Akoi, M.; Taniguchi, S.; Okada, T.; Shirakawa, M.; Sakata, Y. *Chem. Phys. Lett*. **1996**, *263*, 545. (b) Imahori, H.; Tamaki, K.; Guldi, D M.; Luo, C.; Fujitsuka, M.; Ito, O.; Sakata, Y.; Fukuzumi, *J. Am. Chem. Soc*. **2001**, *123*, 2607.

(23) (a) Boulle, C.; Rabreau, J. M.; Hudhomme, P.; Cariou, M.; Jubault, M.; Gorgues, A.; Orduna, J.; Garín, J. *Tetrahedron Lett.* **1997**, *38*, 3909. (b) Hudhomme, P.; Boulle, C.; Rabreau, J. M.; Cariou, M.; Jubault, M.; Gorgues, A. *Synth. Met*. **1998**, *94*, 73 (c) Kreher, D.; Hudhomme, P.; Gorgues, A.; Luo, H.; Araki, Y.; Ito, O. *Phys. Chem. Chem. Phys*. **2003**, *5*, 4583.

(24) Llacay, J.; Veciana, J.; Vidal-Gancedo, J.; Bourdelande, J. L.; Gonzalez-Moreno, R.; Rovira, C. *J. Org. Chem.* **1998**, *63*, 5201.

(25) (a) Allard, E.; Delaunay, J.; Cheng, F.; Cousseau, J.; Ordúna, J.; Garín, J. *Org. Lett.* **2001**, *3*, 3503. (b) Allard, E.; Cousseau, J.; Ordúna, J.; Garín, J.; Luo, H.; Araki, Y.; Ito, O. *Phys. Chem. Chem. Phys.* **2002**, *4*, 5944.

(26) Komamine, S.; Fujitsuka, M.; Ito, O.; Morikawa, K.; Miyata, T.; Ohno, T. *J. Phys. Chem. A* **2000**, *104*, 11497.

(27) (a) Marcus, R. A. *J. Chem. Phys.* **1956**, *24*, 966. (b) Marcus, R. A. *J. Chem. Phys.* **1965**, *43*, 679. (c) Marcus, R. A.; Sutin, N. *Biochim. Biophys. Acta* **1985**, *811*, 265.

(28) (a) Shirota, Y.; Moriwaki, K.; Yoshikawa, S.; Ujike, T.; Nakano, H. *J. Mater. Chem.* **1998**, *8*, 2579. (b) Gauthier, S.; Frechet, J. M. J. *Synthesis* **1987**, 383.

(29) Belik, P.; Gugel, A.; Kraus, A.; Walter, M.; Müllen, K. *J. Org. Chem*. **1995**, *60*, 3307.

(30) Frisch, M. J.; Trucks, G. W.; Schlegel, H. B.; Scuseria, G. E.; Robb, M. A.; Cheeseman, J. R.; Zakrzewski, V. G.; Montgomery, J. A., Jr.; Stratmann, R. E.; Burant, J. C.; Dapprich, S.; Millam, J. M.; Daniels, A. D.; Kudin, K. N.; Strain, M. C.; Farkas, O.; Tomasi, J.; Barone, V.; Cossi, M.; Cammi, R.; Mennucci, B.; Pomelli, C.; Adamo, C.; Clifford, S.; Ochterski, J.; Petersson, G. A.; Ayala, P. Y.; Cui, Q.; Morokuma, K.; Malick, D. K.; Rabuck, A. D.; Raghavachari, K.; Foresman, J. B.; Cioslowski, J.; Ortiz, J. V.; Baboul, A. G.; Stefanov, B. B.; Liu, G.; Liashenko, A.; Piskorz, P.; Komaromi, I.; Gomperts, R.; Martin, R. L.; Fox, D. J.; Keith, T.; Al-Laham, M. A.; Peng, C. Y.; Nanayakkara, A.; Gonzalez, C.; Challacombe, M.; Gill, P. M. W.; Johnson, B.; Chen, W.; Wong, M. W.; Andres, J. L.; Gonzalez, C.; Head-Gordon, M.; Replogle, E. S.; Pople, J. A. *Gaussian 98*, Revision A.7; Gaussian, Inc.: Pittsburgh, PA, 1998.

(31) Weller, A. *Z. Phys. Chem. Neue Folge* **1982**, *133*, 93.

(32) Although from eq 7 two solutions were given for the λ_{CR} values, 0.77 and 2.23 eV in PhCN and 0.87 and 2.44 eV in THF for the λ values of the CR process, we adopted the smaller values.

(33) For C_{60}−BBA with $R_{cc} = 10$ Å, from $\Delta G^{\ddagger S}_{CS} = 0.15$ eV, $\lambda^{S}_{CS} = 0.02$ and 0.62 eV were obtained corresponding to $|V^{S}_{CS}| = 7.93$ and 17.98 cm^{-1} in anisole. In the previous paper,[26] the larger values were discussed; however, the smaller values are also comparable with the values in PhCN evaluated in the present study.

(34) Sandanayaka, A. S. D.; Sasabe, H.; Araki, Y.; Furusho, Y.; Ito, O.; Takata T. *J. Phys. Chem. A* **2004**, *108*, 5145.

(35) (a) Yamanaka, K.; Fujitsuka, M.; Araki, Y.; Ito, O.; Aoshima, T.: Fukushima, T.; Miyashi, T. *J. Phys. Chem. A* **2004**, *108*, 250. (b) Luo, H.; Fujitsuka, M.; Araki, Y.; Ito, O.; Padmawar, P.; Chiang, L. Y. *J. Phys. Chem. B* **2003**, *107*, 9312.

(36) (a) Yamazaki, M.; Araki, Y.; Fujitsuka, M.; Ito, O. *J. Phys. Chem. A* **2001**, *105*, 8615. (b) D'Souza, F.; Deviprasad, G. R.; Zandler, M. E.; Hoang, V. T.; Klykov, A. El-Khouly, M. E.; Fujitsuka, M.; Ito, O. *J. Phys. Chem. B* **2002**, *106*, 4952.